Steel and Composite Structures, *Vol. 34, No. 5 (2020) 733-742*
DOI: https://doi.org/10.12989/scs.2020.34.5.733

The effect of voltage and nanoparticles on the vibration of sandwich nanocomposite smart plates

Ahmad Farrokhian*

Mechanical Engineering group, Pardis College, Isfahan University of Technology, Isfahan 84156-83111, Iran

(*Received October 15, 2019, Revised January 8, 2020, Accepted January 27, 2020*)

Abstract. Vibration analysis in nanocomposite plate with smart layer is studied in this article. The plate is reinforced by carbon nanotubes where the Mori-Tanaka law is utilized for obtaining the effective characteristic of structure assuming agglomeration effects. The nanocomposite plate is located in elastic medium which is simulated by spring element. The motion equations are derived based on first order shear deformation theory and Hamilton's principle. Utilizing Navier method, the frequency of the structure is calculated and the effects of applied voltage, volume percent and agglomeration of Carbon nanotubes, elastic medium and geometrical parameters of structure are shown on the frequency of system. Results indicate that with applying negative voltage, the frequency of structure is increased. In addition, the agglomeration of carbon nanotubes reduces the frequency of the nanocomposite plate.

Keywords: nanocomposite plate; vibration; smart layer; elastic medium; exact method

1. Introduction

Various internal and external loads generate vibration in the mechanical devices. These vibrations also affect the plates performance and however the vibrations can need to be decreased. Vibrations may be decreased by improving the characteristics of plates by new technologies, such as the utilize of piezoelectric materials. In addition, plate can be reinforced by nanoparticles for increasing its stiffness.

The vibration behavior of plates on elastic foundations has attracted considerable attention in recent years. Lam *et al*. (2000) used the Green's functions to obtain canonical exact solutions of elastic bending, buckling and vibration for Levy plates resting on two-parameter elastic foundations. The free vibrations of simply supported rectangular plates, resting on two different models of soils, were considered by De Rosa and Lippiello (2009). Ferreira *et al.* (2010) used the radial basis function collocation method to study static deformation and free vibration of plates on Pasternak foundation. Kumar and Lal (2012) studied the vibration analysis of nonhomogeneous orthotropic rectangular plates with bilinear thickness variation resting on Winkler foundation. Bahmyari and khedmati (2013) considered the vibration analysis of nonhomogeneous moderately thick plates with point supports resting on Pasternak elastic foundation using element free Galerkin method. Vibrational analysis of advanced composite plates resting on elastic foundation was studied by Mantari *et al*. (2014). They derived the governing equations of a type of functionally graded plates resting on elastic foundation by employing the Hamilton's principal. Uğurlu (2016) analyzed the vibration of elastic bottom plates of fluid storage tanks resting on Pasternak foundation based on boundary element method. Also, a dimensionless parametric study for forced vibrations of foundation-soil systems was done by Chen *et al*. (2016). A non-polynomial four variable refined plate theory for free vibration of functionally graded thick rectangular plates on elastic foundation was investigated by Meftah *et al.* (2017). The eigenfrequency responses of a nanoplate structure were evaluated numerically by Mehr *et al*. (2018) via a novel higher-order mathematical model and finite-element method including nonlocal elasticity theory. Microstructure-dependent static stability analysis of inhomogeneous tapered micro-columns was performed by Akgöz (2019). Medani *et al.* (2019) studied static and dynamic behavior of Functionally Graded Carbon Nanotubes (FG-CNT)-reinforced porous sandwich (PMPV) polymer plate. Thermal buckling temperature values of the graded carbon nanotube reinforced composite shell structure was explored by Mehar and panda (2019)

using higher-order mid-plane kinematics and multiscale constituent modeling under two different thermal fields.

None of the above researchers have considered piezo-based nano-composite structures. Numerical analysis of large amplitude free vibration behaviour of laminated composite spherical shell panel embedded with the piezoelectric layer was presented by Singh and Panda (2015a). The nonlinear free vibration behaviour of laminated composite single/doubly curved shell panel embedded with the piezoelectric layer was investigated numerically by Singh and Panda (2015a). Singh and Panda (2016) investigated the geometrical nonlinear free vibration characteristic of cylindrical composite shell panel embedded with piezoelectric layers. Static Piezo-based

*Corresponding author, Ph.D.
E-mail: ahmadfarrokhian@yahoo.com

ISSN: 1229-9367 (Print), 1598-6233 (Online)

wireless sensor network for early-age concrete strength monitoring is planned by Chen *et al.* (2016). The geometrically nonlinear transient response of the smart laminated composite plate was investigated by Singh *et al.* (2016a) under the coupled electromechanical load. Singh *et al.* (2016b) studied geometrical nonlinear flexural behaviour of laminated composite shell panels integrated with the piezoelectric fibre reinforced composite (PFRC) layer. Sasmal *et al.* (2017) investigated electrical conductivity and piezo-resistive characteristics of CNT and CNF incorporated cementitious nanocomposites under static and dynamic loading. The flexural behaviour of the laminated composite plate embedded with two different smart materials (piezoelectric and magnetostrictive) and subsequent deflection suppression were investigated by Dutta *et al.* (2017). Static bending and strength behaviour of the laminated composite plate embedded with magnetostrictive (MS) material was computed numerically by Suman *et al.* (2017). Chahar and Kumar (2019) studied the effect of ply orientation and control gain on tip transverse displacement of functionally graded beam layer for both active constrained layer damping (ACLD) and passive constrained layer damping (PCLD) system.

The purpose of this paper is to study the free vibration and smart control of plate reinforced by carbon nanotubes embedded in elastic medium. The structure is covered by a piezoelectric layer subjected to external voltage. In order to obtain the equivalent material properties of nanocomposite structure, the Mori-Tanaka model is used. Applying first order shear deformation theory, the motion equations are achieved based on Hamilton's principal. Navier method is applied for obtaining the frequency of the system. The effects of applied voltage, volume percent and agglomeration of carbon nanotubes, elastic medium and geometrical parameters of structure on the frequency of system are disused in detail.

2. Mathematical model

As shown in Fig. 1, a plate reinforced with Carbon nanotubes and covered by piezoelectric layer with length L, width b, thickness h and piezoelectric layer thickness h_p is considered.

Since, the structure of this paper is a flat plate, the FSDT is chosen. In addition, this theory, predicts the accurate results considering shear correction factor for flat plates

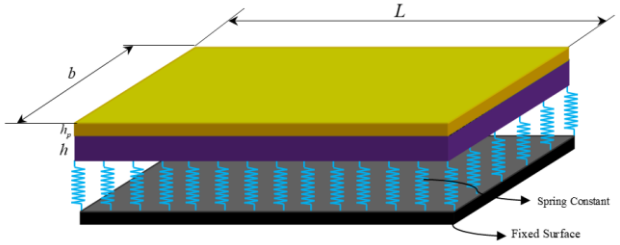

Fig. 1 A schematic figure for plate with piezoelectric layers reinforced with Carbon nanotubes

(Hosseini-Hashemi *et al.* 2010). Based on FSDT plate theory, the displacement field can be expressed as (Reddy 2003)

$$u(x,y,z,t)=u(x,y,t)+z\phi_x(x,y,t), \quad (1a)$$

$$v(x,y,z,t)=v(x,y,t)+z\phi_y(x,y,t), \quad (1b)$$

$$w(x,y,z,t)=w(x,y,t), \quad (1c)$$

where ($u(x,y,z,t), v(x,y,z,t), w(x,y,z,t)$) denote the displacement components at an arbitrary point (x,y,z) in the plate, and ($u(x,y,t), v(x,y,t), w(x,y,t)$) are the displacement of a material point at (x, y) on the mid-plane (i.e., $z=0$) of the plate along the x-, y -, and z-directions, respectively; ϕ_x and φ_y are the rotations of the normal to the mid-plane about x- and y - directions, respectively. Based on above relations, the strain-displacement equations may be written as

$$\varepsilon_{xx}=\frac{\partial u}{\partial x}+z\frac{\partial \phi_x}{\partial x}, \quad (2a)$$

$$\varepsilon_{yy}=\frac{\partial v}{\partial y}+z\frac{\partial \phi_y}{\partial y}, \quad (2b)$$

$$\gamma_{xy}=\frac{\partial v}{\partial x}+\frac{\partial u}{\partial y}+z\left(\frac{\partial \phi_y}{\partial x}+\frac{\partial \phi_x}{\partial y}\right), \quad (2c)$$

$$\gamma_{xz}=\phi_x+\frac{\partial w}{\partial x}, \quad (2d)$$

$$\gamma_{zy}=\frac{\partial w}{\partial y}+\phi_y. \quad (2e)$$

where $(\varepsilon_{xx}, \varepsilon_{yy})$ are the normal strain components and $(\gamma_{yz}, \gamma_{xz}, \gamma_{xy})$ are the shear strain components.

The constitutive equation for stresses $\boldsymbol{\sigma}$ and strains $\boldsymbol{\varepsilon}$ matrix on the mechanical side, as well as flux density $\mathbf{D}$ and field strength $\mathbf{E}$ matrix on the electrostatic side, may be arbitrarily combined as follows (Kolahchi *et al.* 2016)

$$\begin{Bmatrix}\sigma_{xx}\\ \sigma_{yy}\\ \tau_{yz}\\ \tau_{xz}\\ \tau_{xy}\end{Bmatrix}=\begin{bmatrix}C_{11} & C_{12} & 0 & 0 & 0\\ C_{21} & C_{22} & 0 & 0 & 0\\ 0 & 0 & C_{44} & 0 & 0\\ 0 & 0 & 0 & C_{55} & 0\\ 0 & 0 & 0 & 0 & C_{66}\end{bmatrix}\begin{Bmatrix}\varepsilon_{xx}\\ \varepsilon_{yy}\\ \gamma_{yz}\\ \gamma_{xz}\\ \gamma_{xy}\end{Bmatrix}-\begin{bmatrix}0 & 0 & e_{31}\\ 0 & 0 & e_{32}\\ 0 & e_{24} & 0\\ e_{15} & 0 & 0\\ 0 & 0 & 0\end{bmatrix}\begin{Bmatrix}E_x\\ E_y\\ E_z\end{Bmatrix}, \quad (3)$$

$$\begin{Bmatrix}D_x\\ D_y\\ D_z\end{Bmatrix}=\begin{bmatrix}0 & 0 & 0 & e_{15} & 0\\ 0 & 0 & e_{24} & 0 & 0\\ e_{31} & e_{32} & 0 & 0 & 0\end{bmatrix}\begin{Bmatrix}\varepsilon_{xx}\\ \varepsilon_{yy}\\ \gamma_{yz}\\ \gamma_{xz}\\ \gamma_{xy}\end{Bmatrix}+\begin{bmatrix}\epsilon_{11} & 0 & 0\\ 0 & \epsilon_{22} & 0\\ 0 & 0 & \epsilon_{33}\end{bmatrix}\begin{Bmatrix}E_x\\ E_y\\ E_z\end{Bmatrix}, \quad (4)$$

where σ_{ij}, ε_{ij}, D_{ii} and E_{ii} are stress, strain, electric displacement and electric field, respectively. Also, C_{ij}, e_{ij} and $\in_{ij}$ denote elastic, piezoelectric and dielectric coefficients, respectively. Noted that C_{ij} may be obtained using Mori-Tanaka model (Mori and Tanaka 1973). The electric field in terms of electric potential (Φ) is expressed as

$$E_k = -\nabla\Phi, \tag{5}$$

where, the electric potential is assumed as the combination of a half-cosine and linear variation, which satisfies the Maxwell equation. It can be written as (Kolahchi *et al.* 2016)

$$\Phi(x,y,z,t) = -\cos(\frac{\pi z}{h})\varphi(x,y,t) + \frac{2V_0 z}{h}, \tag{6}$$

where $\phi(x,\theta,t)$ is the time and spatial distribution of the electric potential which must satisfy the electric boundary conditions, V_0 is external electric voltage. However, using Eq. (1), the governing equations of piezoelectric material (i.e., Eqs. (3) and (4)) for FSDT may be written as

$$\sigma_{xx}^{p} = C_{11}\varepsilon_{xx} + C_{12}\varepsilon_{yy} + e_{31}\left(\frac{\pi}{h}\sin\left(\frac{\pi z}{h}\right)\varphi + \frac{2V_0}{h}\right), \tag{7}$$

$$\sigma_{yy}^{p} = C_{12}\varepsilon_{xx} + C_{22}\varepsilon_{yy} + e_{32}\left(\frac{\pi}{h}\sin\left(\frac{\pi z}{h}\right)\varphi + \frac{2V_0}{h}\right), \tag{8}$$

$$\tau_{yz}^{p} = C_{44}\gamma_{yz} - e_{24}\left(\cos\left(\frac{\pi z}{h}\right)\frac{\partial\varphi}{\partial y}\right), \tag{9}$$

$$\tau_{xz}^{p} = C_{55}\gamma_{zx} - e_{15}\left(\cos\left(\frac{\pi z}{h}\right)\frac{\partial\varphi}{\partial x}\right), \tag{10}$$

$$\tau_{xy}^{p} = C_{66}\gamma_{xy}, \tag{11}$$

$$D_x = e_{15}\gamma_{xz} + \in_{11}\left(\cos\left(\frac{\pi z}{h}\right)\frac{\partial\varphi}{\partial y}\right), \tag{12}$$

$$D_y = e_{24}\gamma_{zy} + \in_{22}\left(\cos\left(\frac{\pi z}{h}\right)\frac{\partial\varphi}{\partial y}\right), \tag{13}$$

$$D_z = e_{31}\varepsilon_{xx} + e_{32}\varepsilon_{yy} - \in_{33}\left(\frac{\pi}{h}\sin\left(\frac{\pi z}{h}\right)\varphi + \frac{2V_0}{h}\right). \tag{14}$$

For the plate, with neglecting the piezoelectric properties we have

$$\sigma_{xx}^{c} = Q_{11}\varepsilon_{xx} + Q_{12}\varepsilon_{yy}, \tag{15}$$

$$\sigma_{yy}^{c} = Q_{12}\varepsilon_{xx} + Q_{22}\varepsilon_{yy}, \tag{16}$$

$$\tau_{yz}^{c} = Q_{44}\gamma_{yz}, \tag{17}$$

$$\tau_{xz}^{c} = Q_{55}\gamma_{zx}, \tag{18}$$

$$\tau_{xy}^{c} = Q_{66}\gamma_{xy}, \tag{19}$$

2.1 Mori-Tanaka Model and agglomeration effects

In this section, the effective modulus of the plate reinforced by Carbon nanotubes is developed. Different methods are available to obtain the average properties of a composite. Due to its simplicity and accuracy even at high volume fractions of the inclusions, the Mori-Tanaka method is employed in this section. The matrix is assumed to be isotropic and elastic, with the Young's modulus E_m and the Poisson's ratio υ_m. The constitutive relations for a layer of the composite with the principal axes parallel to the x-, y- and z directions are (Mori and Tanaka 1973)

$$\begin{Bmatrix}\sigma_{11}\\ \sigma_{22}\\ \sigma_{33}\\ \sigma_{23}\\ \sigma_{13}\\ \sigma_{12}\end{Bmatrix} = \begin{bmatrix} k+m & l & k-m & 0 & 0 & 0\\ l & n & l & 0 & 0 & 0\\ k-m & l & k+m & 0 & 0 & 0\\ 0 & 0 & 0 & p & 0 & 0\\ 0 & 0 & 0 & 0 & m & 0\\ 0 & 0 & 0 & 0 & 0 & p \end{bmatrix}\begin{Bmatrix}\varepsilon_{11}\\ \varepsilon_{22}\\ \varepsilon_{33}\\ \gamma_{23}\\ \gamma_{13}\\ \gamma_{12}\end{Bmatrix} \tag{20}$$

where $\sigma_{ij}, \varepsilon_{ij}, \gamma_{ij}, k, m, n, l, p$ are the stress components, the strain components and the stiffness coefficients respectively. According to the Mori-Tanaka method the stiffness coefficients are given by

$$\begin{aligned}
k &= \frac{E_m\{E_m c_m + 2k_r(1+\nu_m)[1+c_r(1-2\nu_m)]\}}{2(1+\nu_m)[E_m(1+c_r-2\nu_m)+2c_m k_r(1-\nu_m-2\nu_m^2)]}\\
l &= \frac{E_m\{c_m\nu_m[E_m+2k_r(1+\nu_m)]+2c_r l_r(1-\nu_m^2)]\}}{(1+\nu_m)[E_m(1+c_r-2\nu_m)+2c_m k_r(1-\nu_m-2\nu_m^2)]}\\
n &= \frac{E_m^2 c_m(1+c_r-c_m\nu_m)+2c_m c_r(k_r n_r - l_r^2)(1+\nu_m)^2(1-2\nu_m)}{(1+\nu_m)[E_m(1+c_r-2\nu_m)+2c_m k_r(1-\nu_m-2\nu_m^2)]}\\
&\quad + \frac{E_m[2c_m^2 k_r(1-\nu_m)+c_r n_r(1+c_r-2\nu_m)-4c_m l_r\nu_m]}{E_m(1+c_r-2\nu_m)+2c_m k_r(1-\nu_m-2\nu_m^2)}\\
p &= \frac{E_m[E_m c_m + 2p_r(1+\nu_m)(1+c_r)]}{2(1+\nu_m)[E_m(1+c_r)+2c_m p_r(1+\nu_m)]}\\
m &= \frac{E_m[E_m c_m + 2m_r(1+\nu_m)(3+c_r-4\nu_m)]}{2(1+\nu_m)\{E_m[c_m+4c_r(1-\nu_m)]+2c_m m_r(3-\nu_m-4\nu_m^2)\}}
\end{aligned} \tag{21}$$

where the subscripts m and r stand for matrix and reinforcement respectively. C_m and C_r are the volume fractions of the matrix and the nanoparticles respectively and k_r, l_r, n_r, p_r, m_r are the Hills elastic modulus for the nanoparticles (Mori and Tanaka 1973). The experimental results show that the assumption of uniform dispersion for nanoparticles in the matrix is not correct and the most of nanoparticles are bent and centralized in one area of the matrix. These regions with concentrated nanoparticles are assumed to have spherical shapes, and are considered as "inclusions" with different elastic properties from the surrounding material. The total volume V_r of

nanoparticles can be divided into the following two parts (Shi and Feng 2004)

$$V_r = V_r^{inclusion} + V_r^m \tag{22}$$

where $V_r^{inclusion}$ and V_r^m are the volumes of nanoparticles dispersed in the spherical inclusions and in the matrix, respectively. Introduce two parameters ξ and ζ describe the agglomeration of nanoparticles

$$\xi = \frac{V_{inclusion}}{V}, \tag{23}$$

$$\zeta = \frac{V_r^{inclusion}}{V_r}. \tag{24}$$

However, the average volume fraction c_r of nanoparticles in the composite is

$$c_r = \frac{V_r}{V}. \tag{25}$$

Assume that all the orientations of the nanoparticles are completely random. Hence, the effective bulk modulus (K) and effective shear modulus (G) may be written as

$$K = K_{out}\left[1+\frac{\xi\left(\frac{K_{in}}{K_{out}}-1\right)}{1+\alpha\left(1-\xi\right)\left(\frac{K_{in}}{K_{out}}-1\right)}\right], \tag{26}$$

$$G = G_{out}\left[1+\frac{\xi\left(\frac{G_{in}}{G_{out}}-1\right)}{1+\beta\left(1-\xi\right)\left(\frac{G_{in}}{G_{out}}-1\right)}\right], \tag{27}$$

where

$$K_{in} = K_m + \frac{\left(\delta_r - 3K_m\chi_r\right)c_r\zeta}{3\left(\xi - c_r\zeta + c_r\zeta\chi_r\right)}, \tag{28}$$

$$K_{out} = K_m + \frac{c_r\left(\delta_r - 3K_m\chi_r\right)\left(1-\zeta\right)}{3\left[1-\xi-c_r\left(1-\zeta\right)+c_r\chi_r\left(1-\zeta\right)\right]}, \tag{29}$$

$$G_{in} = G_m + \frac{\left(\eta_r - 3G_m\beta_r\right)c_r\zeta}{2\left(\xi - c_r\zeta + c_r\zeta\beta_r\right)}, \tag{30}$$

$$G_{out} = G_m + \frac{c_r\left(\eta_r - 3G_m\beta_r\right)\left(1-\zeta\right)}{2\left[1-\xi-c_r\left(1-\zeta\right)+c_r\beta_r\left(1-\zeta\right)\right]}, \tag{31}$$

where $\chi_r, \beta_r, \delta_r, \eta_r$ may be calculated as

$$\chi_r = \frac{3\left(K_m + G_m\right) + k_r - l_r}{3\left(k_r + G_m\right)}, \tag{32}$$

$$\beta_r = \frac{1}{5}\left\{\frac{4G_m + 2k_r + l_r}{3\left(k_r + G_m\right)} + \frac{4G_m}{\left(p_r + G_m\right)} + \frac{2\left[G_m\left(3K_m + G_m\right) + G_m\left(3K_m + 7G_m\right)\right]}{G_m\left(3K_m + G_m\right) + m_r\left(3K_m + 7G_m\right)}\right\}, \tag{33}$$

$$\delta_r = \frac{1}{3}\left[n_r + 2l_r + \frac{\left(2k_r - l_r\right)\left(3K_m + 2G_m - l_r\right)}{k_r + G_m}\right], \tag{34}$$

$$\eta_r = \frac{1}{5}\left[\frac{2}{3}\left(n_r - l_r\right) + \frac{8G_m m_r\left(3K_m + 4G_m\right)}{3K_m\left(m_r + G_m\right) + G_m\left(7m_r + G_m\right)} + \frac{4G_m p_r}{\left(p_r + G_m\right)} + \frac{2\left(k_r - l_r\right)\left(2G_m + l_r\right)}{3\left(k_r + G_m\right)}\right]. \tag{35}$$

where, K_m and G_m are the bulk and shear moduli of the matrix which can be written as

$$K_m = \frac{E_m}{3\left(1-2\upsilon_m\right)}, \tag{36}$$

$$G_m = \frac{E_m}{2\left(1+\upsilon_m\right)}. \tag{37}$$

Furthermore, β, α can be obtained from

$$\alpha = \frac{\left(1+\upsilon_{out}\right)}{3\left(1-\upsilon_{out}\right)}, \tag{38}$$

$$\beta = \frac{2\left(4-5\upsilon_{out}\right)}{15\left(1-\upsilon_{out}\right)}, \tag{39}$$

$$\upsilon_{out} = \frac{3K_{out} - 2G_{out}}{6K_{out} + 2G_{out}}. \tag{40}$$

Finally, the elastic modulus (E) and poison's ratio (υ) can be calculated as

$$E = \frac{9KG}{3K + G}, \tag{41}$$

$$\upsilon = \frac{3K - 2G}{6K + 2G}. \tag{42}$$

2.2 Energy method

The potential energy can be written as

$$U = \frac{1}{2}\int\begin{pmatrix}\sigma_{xx}^c\varepsilon_{xx} + \sigma_{yy}^c\varepsilon_{yy} + \tau_{xz}^c\gamma_{xz} + \tau_{yz}^c\gamma_{yz} + \tau_{xy}^c\gamma_{xy}\\ +\sigma_{xx}^p\varepsilon_{xx} + \sigma_{yy}^p\varepsilon_{yy} + \tau_{xz}^p\gamma_{xz} + \tau_{yz}^p\gamma_{yz} + \tau_{xy}^p\gamma_{xy}\\ -D_xE_x - D_yE_y - D_zE_z\end{pmatrix}dV, \tag{43}$$

Combining of Eqs. (1), (7)-(14) and (43) yields

$$U=\frac{1}{2}\int_0^b\int_0^L\left\{\left[N_{xx}\frac{\partial u}{\partial x}+M_{xx}\frac{\partial \phi_x}{\partial x}\right]+\left[N_{yy}\frac{\partial v}{\partial y}+M_{yy}\frac{\partial \phi_y}{\partial y}\right]\right.$$
$$+Q_x\left(\phi_x+\frac{\partial w}{\partial x}\right)+N_{xy}\left[\frac{\partial v}{\partial x}+\frac{\partial u}{\partial y}\right]+M_{xy}\left[\frac{\partial \phi_y}{\partial x}+\frac{\partial \phi_x}{\partial y}\right]Rxdy$$
$$+Q_y\left[\frac{\partial w}{\partial y}+\phi_y\right]+\int_{-h/2}^{h/2+h_p}\int_0^b\int_0^L -D_x\left[\cos\left(\frac{\pi z}{h}\right)\frac{\partial \varphi}{\partial x}\right] \quad (44)$$
$$\left.-D_y\left[\cos\left(\frac{\pi z}{h}\right)\frac{\partial \varphi}{\partial y}\right]-D_z\left[-\frac{\pi}{h}\sin\left(\frac{\pi z}{h}\right)\varphi-\frac{2V_0}{h}\right]\right\}dxdydz,$$

where the stress resultant-displacement relations can be written as

$$\begin{Bmatrix}N_{xx}\\N_{yy}\\N_{xy}\end{Bmatrix}=\int_{-\frac{h}{2}}^{\frac{h}{2}}\begin{Bmatrix}\sigma_{xx}^c\\\sigma_{yy}^c\\\tau_{xy}^c\end{Bmatrix}dz+\int_{\frac{h}{2}}^{\frac{h}{2}+h_p}\begin{Bmatrix}\sigma_{xx}^p\\\sigma_{yy}^p\\\tau_{xy}^p\end{Bmatrix}dz \quad (45)$$

$$\begin{Bmatrix}Q_x\\Q_y\end{Bmatrix}=k'\int_{-\frac{h}{2}}^{\frac{h}{2}}\begin{Bmatrix}\tau_{xz}^c\\\tau_{yz}^c\end{Bmatrix}dz+k'\int_{-\frac{h}{2}}^{\frac{h}{2}+h_p}\begin{Bmatrix}\tau_{xz}^p\\\tau_{yz}^p\end{Bmatrix}dz, \quad (46)$$

$$\begin{Bmatrix}M_{xx}\\M_{yy}\\M_{xy}\end{Bmatrix}=\int_{-\frac{h}{2}}^{\frac{h}{2}}\begin{Bmatrix}\sigma_{xx}^c\\\sigma_{yy}^c\\\tau_{xy}^c\end{Bmatrix}z\,dz+\int_{\frac{h}{2}}^{\frac{h}{2}+h_p}\begin{Bmatrix}\sigma_{xx}^p\\\sigma_{yy}^p\\\tau_{xy}^p\end{Bmatrix}zdz, \quad (47)$$

In which k' is shear correction coefficient. Substituting Eqs. (1) and (7)-(14) into Eqs. (45)-(47), the stress resultant-displacement relations can be obtained as follow

$$N_{xx}=A_{110}\frac{\partial u}{\partial x}+A_{111}\frac{\partial \phi_x}{\partial x}+A_{120}\frac{\partial v}{\partial y}+A_{121}\frac{\partial \phi_y}{\partial y}+E_{31}\varphi, \quad (48)$$

$$N_{yy}=A_{120}\frac{\partial u}{\partial x}+A_{121}\frac{\partial \phi_x}{\partial x}+A_{220}\frac{\partial v}{\partial y}+A_{221}\frac{\partial \phi_y}{\partial y}+E_{32}\varphi, \quad (49)$$

$$Q_y=k'A_{44}\left[\frac{\partial w}{\partial y}+\phi_y\right]+E_{24}\frac{\partial \varphi}{\partial y}, \quad (50)$$

$$Q_x=k'A_{55}\left(\frac{\partial w}{\partial x}+\phi_x\right)+E_{15}\frac{\partial \varphi}{\partial x}, \quad (51)$$

$$N_{xy}=A_{660}\left(\frac{\partial u}{\partial y}+\frac{\partial v}{\partial x}\right)+A_{661}\left(\frac{\partial \phi_x}{\partial y}+\frac{\partial \phi_y}{\partial x}\right), \quad (52)$$

$$M_{xx}=A_{111}\frac{\partial u}{\partial x}+A_{112}\frac{\partial \phi_x}{\partial x}+A_{121}\frac{\partial v}{\partial y}+A_{122}\frac{\partial \phi_y}{\partial y}+F_{31}\varphi, \quad (53)$$

$$M_{yy}=A_{121}\frac{\partial u}{\partial x}+A_{122}\frac{\partial \phi_x}{\partial x}+A_{221}\frac{\partial v}{\partial y}+A_{222}\frac{\partial \phi_y}{\partial y}+F_{32}\varphi, \quad (54)$$

$$M_{xy}=A_{661}\left(\frac{\partial u}{\partial y}+\frac{\partial v}{\partial x}\right)+A_{662}\left(\frac{\partial \phi_x}{\partial y}+\frac{\partial \phi_y}{\partial x}\right), \quad (55)$$

Where

$$A_{11k}=\int_{-h/2}^{h/2}Q_{11}z^k dz+\int_{-h/2}^{h/2+h_p}C_{11}z^k dz, \qquad k=0,1,2 \quad (56)$$

$$A_{12k}=\int_{-h/2}^{h/2}Q_{12}z^k dz+\int_{-h/2}^{h/2+h_p}C_{12}z^k dz, \qquad k=0,1,2 \quad (57)$$

$$A_{22k}=\int_{-h/2}^{h/2}Q_{22}z^k dz+\int_{-h/2}^{h/2+h_p}C_{22}z^k dz, \qquad k=0,1,2 \quad (58)$$

$$A_{66k}=\int_{-h/2}^{h/2}Q_{66}z^k dz+\int_{-h/2}^{h/2+h_p}C_{66}z^k dz, \qquad k=0,1,2 \quad (59)$$

$$A_{44}=\int_{-h/2}^{h/2}Q_{44}dz+\int_{-h/2}^{h/2+h_p}C_{44}dz, \quad (60)$$

$$A_{55}=\int_{-h/2}^{h/2}Q_{55}dz+\int_{-h/2}^{h/2+h_p}C_{55}dz, \quad (61)$$

$$(E_{31},E_{32})=\frac{\pi}{h}\int_{-h/2}^{h/2}(e_{31},e_{32})\sin\left(\frac{\pi z}{h}\right)dz, \quad (62)$$

$$(E_{24},E_{15})=-\int_{-h/2}^{h/2}(e_{24},e_{15})\cos\left(\frac{\pi z}{h}\right)dz, \quad (63)$$

$$(F_{31},F_{32})=\frac{\pi}{h}\int_{-h/2}^{h/2}(e_{31},e_{32})\sin\left(\frac{\pi z}{h}\right)zdz, \quad (64)$$

The kinetic energy of system may be written as

$$K=\frac{(\rho^c+\rho^p)}{2}\int\left(\left(\frac{\partial u}{\partial t}+z\frac{\partial \phi_x}{\partial t}\right)^2+\left(\frac{\partial v}{\partial t}+z\frac{\partial \phi_y}{\partial t}\right)^2+\left(\frac{\partial w}{\partial t}\right)^2\right)dV. \quad (65)$$

in which the density of nanocomposite plate based on Mori-Tanak model can be obtained from $\rho^c=c_r\rho_r+(1-c_r)\rho_m$ where ρ_r and ρ_m are density of nanoparticles and plate, respectively. Defining the moments of inertia as below

$$\begin{Bmatrix}I_0\\I_1\\I_2\end{Bmatrix}=\int_{-h/2}^{h/2}\begin{bmatrix}\rho^c\\\rho^c z\\\rho^c z^2\end{bmatrix}dz+\int_{h/2}^{h/2+h_p}\begin{bmatrix}\rho^p\\\rho^p z\\\rho^p z^2\end{bmatrix}dz, \quad (66)$$

the kinetic energy may be written as

$$K=\frac{1}{2}\int\left(I_0\left(\left(\frac{\partial u}{\partial t}\right)^2+\left(\frac{\partial v}{\partial t}\right)^2+\left(\frac{\partial w}{\partial t}\right)^2\right)+I_1\left(2\frac{\partial u}{\partial t}\frac{\partial \phi_x}{\partial t}+2\frac{\partial v}{\partial t}\frac{\partial \phi_y}{\partial t}\right)\right.$$
$$\left.+I_2\left(\left(\frac{\partial \phi_x}{\partial t}\right)^2+\left(\frac{\partial \phi_y}{\partial t}\right)^2\right)\right)dA, \quad (67)$$

The external work due to elastic medium can be written as (Bowles 1988)

$$W_e=\int_0^{2\pi}\int_0^L(-K_w w)dxdy, \quad (68)$$

where K_w is Winkler's spring modulus. In addition, the in-plane forces may be written as

$$W_f = -\frac{1}{2}\int\left[N^f_{xx}\left(\frac{\partial w}{\partial x}\right)^2 + N^f_{yy}\left(\frac{\partial w}{\partial y}\right)^2\right]dxdy. \quad (69)$$

where

$$N^f_{xx} = N^M_{xx} + N^E_{xx} = N^M_{xx} + 2V_0 e_{31}, \quad (70)$$

$$N^f_{yy} = N^M_{yy} + N^E_{yy} = N^M_{yy} + 2V_0 e_{32}. \quad (71)$$

The governing equations can be derived by Hamilton's principal as follows

$$\int_0^t (\delta U - \delta K - \delta W_e - \delta W_f)dt = 0. \quad (72)$$

Substituting Eqs. (42), (67), (68) and (71) into Eq. (72) yields the following governing equations

$$\delta u: \frac{\partial N_{xx}}{\partial x} + \frac{\partial N_{xy}}{\partial y} = I_0\frac{\partial^2 u}{\partial t^2} + I_1\frac{\partial^2 \phi_x}{\partial t^2}, \quad (73)$$

$$\delta v: \frac{\partial N_{xy}}{\partial x} + \frac{\partial N_{yy}}{\partial y} = I_0\frac{\partial^2 v}{\partial t^2} + I_1\frac{\partial^2 \phi_y}{\partial t^2}, \quad (74)$$

$$\delta w: \frac{\partial Q_x}{\partial x} + \frac{\partial Q_y}{\partial y} + N^f_{xx}\frac{\partial^2 w}{\partial x^2} + N^f_{yy}\frac{\partial^2 w}{\partial y^2} - K_w w = I_0\frac{\partial^2 w}{\partial t^2}, \quad (75)$$

$$\delta\phi_x: \frac{\partial M_{xx}}{\partial x} + \frac{\partial M_{xy}}{\partial y} - Q_x = I_2\frac{\partial^2 \phi_x}{\partial t^2} + I_1\frac{\partial^2 u}{\partial t^2}, \quad (76)$$

$$\delta\varphi_y: \frac{\partial M_{xy}}{\partial x} + \frac{\partial M_{xx}}{\partial y} - Q_y = I_2\frac{\partial^2 \phi_y}{\partial t^2} + I_1\frac{\partial^2 v}{\partial t^2}, \quad (77)$$

$$\delta\varphi: \int_{-h/2}^{h/2}\left\{\left[\cos\left(\frac{\pi z}{h}\right)\frac{\partial D_x}{\partial x}\right] + \left[\cos\left(\frac{\pi z}{h}\right)\frac{\partial D_y}{\partial y}\right] + D_z\left[\frac{\pi}{h}\sin\left(\frac{\pi z}{h}\right)\right]\right\}dz = 0 \quad (78)$$

Substituting Eqs. (48) to (55) into Eqs. (73) to (78), the governing equations can be written as follow

$$A_{110}\frac{\partial^2 u}{\partial x^2} + A_{111}\frac{\partial^2 \phi_x}{\partial x^2} + A_{120}\frac{\partial^2 v}{\partial y\,\partial x} + A_{121}\frac{\partial^2 \phi_y}{\partial y\,\partial x} + E_{31}\frac{\partial \varphi}{\partial x} + A_{120}\frac{\partial^2 u}{\partial x\,\partial y} + A_{121}\frac{\partial^2 \phi_x}{\partial x\,\partial y} + A_{220}\frac{\partial^2 v}{\partial y^2} + A_{221}\frac{\partial^2 \phi_y}{\partial y^2} + E_{32}\frac{\partial \varphi}{\partial y} = I_0\frac{\partial^2 u}{\partial t^2} + I_1\frac{\partial^2 \phi_x}{\partial t^2}, \quad (79)$$

$$A_{120}\frac{\partial^2 u}{\partial x\,\partial y} + A_{121}\frac{\partial^2 \phi_x}{\partial x\,\partial y} + A_{220}\frac{\partial^2 v}{\partial y^2} + A_{221}\frac{\partial^2 \phi}{\partial y^2} + E_{32}\frac{\partial \varphi}{\partial y} + A_{660}\left(\frac{\partial^2 u}{\partial y\,\partial x} + \frac{\partial^2 v}{\partial x^2}\right) + A_{661}\left(\frac{\partial^2 \phi_x}{\partial y\,\partial x} + \frac{\partial^2 \phi_y}{\partial x^2}\right) = I_0\frac{\partial^2 v}{\partial t^2} + I_1\frac{\partial^2 \phi_y}{\partial t^2}, \quad (80)$$

$$k'A_{44}\left[\frac{\partial w}{\partial y^2} + \frac{\partial \phi_y}{\partial y}\right] + E_{15}\frac{\partial \varphi}{\partial y^2} + k'A_{55}\left(\frac{\partial^2 w}{\partial x^2} + \frac{\partial \phi_x}{\partial x}\right) + E_{24}\frac{\partial^2 \varphi}{\partial x^2} - A_{120}\frac{\partial u}{\partial x} - A_{121}\frac{\partial \phi_x}{\partial x} - A_{220}\left(\frac{\partial v}{\partial y}\right) - A_{221}\frac{\partial \phi}{\partial y} + N^f_{xx}\frac{\partial^2 w}{\partial x^2} + N^f_{yy}\frac{\partial^2 w}{\partial y^2} - K_w w = I_0\frac{\partial^2 w}{\partial t^2}, \quad (81)$$

$$A_{111}\frac{\partial^2 u}{\partial x^2} + A_{112}\frac{\partial^2 \phi_x}{\partial x^2} + A_{121}\left(\frac{\partial^2 v}{\partial y\,\partial x} + \frac{\partial w}{\partial x}\right) + A_{122}\frac{\partial^2 \phi_y}{\partial y} + F_{31}\frac{\partial \phi}{\partial x} + A_{661}\left(\frac{\partial^2 u}{\partial y^2} + \frac{\partial^2 v}{\partial x\,\partial y}\right) + A_{662}\left(\frac{\partial^2 \phi_x}{\partial y^2} + \frac{\partial^2 \phi_y}{\partial x\,\partial y}\right) - k'A_{55}\left(\frac{\partial w}{\partial x} + \phi_x\right) - E_{15}\frac{\partial \varphi}{\partial x} = I_2\frac{\partial^2 \phi_x}{\partial t^2} + I_1\frac{\partial^2 u}{\partial t^2}, \quad (82)$$

$$A_{121}\frac{\partial^2 u}{\partial x\,\partial y} + A_{122}\frac{\partial^2 \phi_x}{\partial x\,\partial y} + A_{221}\left(\frac{\partial^2 v}{\partial y^2} + \frac{\partial w}{\partial y}\right) + A_{222}\frac{\partial^2 \phi_\theta}{\partial y^2} + F_{32}\frac{\partial \varphi}{\partial y} + A_{661}\left(\frac{\partial^2 u}{\partial y\,\partial x} + \frac{\partial^2 v}{\partial x^2}\right) + A_{662}\left(\frac{\partial^2 \phi_x}{\partial y\,\partial x} + \frac{\partial^2 \phi_y}{\partial x^2}\right) - k'A_{44}\left[\frac{\partial w}{\partial y} + \phi_y\right] - E_{24}\frac{\partial \varphi}{\partial y} = I_2\frac{\partial^2 \phi_y}{\partial t^2} + I_1\frac{\partial^2 v}{\partial t^2}, \quad (83)$$

$$\delta\phi: -E_{15}\left(\frac{\partial \phi_x}{\partial x} + \frac{\partial^2 w}{\partial x^2}\right) + \Xi_{11}\left(\frac{\partial^2 \varphi}{\partial x\,\partial y}\right) - E_{24}\left(\frac{\partial^2 w}{\partial y^2} + \frac{\partial \phi_y}{\partial y}\right) + \Xi_{22}\left(\frac{\partial^2 \varphi}{\partial y^2}\right) + E_{31}\frac{\partial u}{\partial x} + F_{31}\frac{\partial \phi_x}{\partial x} + \frac{E_{32}}{R}\left(w + \frac{\partial v}{\partial y}\right) + F_{32}\frac{\partial \phi_y}{\partial y} - \Xi_{33}\varphi = 0. \quad (84)$$

where

$$(\Xi_{11}, \Xi_{22}) = \int_{-h/2}^{h/2}(\in_{11}, \in_{22})\cos^2\left(\frac{\pi z}{h}\right)dz, \quad (85)$$

$$(\Xi_{33}) = \frac{\pi^2}{h^2}\int_{-h/2}^{h/2}(\in_{33})\sin^2\left(\frac{\pi z}{h}\right)dz. \quad (86)$$

3. Solution procedure

Steady state solutions to the governing equations of the system motion and the electric potential distribution which relate to the simply supported boundary conditions and zero electric potential along the edges of the surface electrodes

can be assumed as

$$u(x,y,t)=u_0\cos(\frac{n\pi x}{L})\sin(\frac{m\pi y}{b})e^{i\omega t}, \quad (87)$$

$$v(x,y,t)=v_0\sin(\frac{n\pi x}{L})\cos(\frac{m\pi y}{b})e^{i\omega t}, \quad (88)$$

$$w(x,y,t)=w_0\sin(\frac{n\pi x}{L})\sin(\frac{m\pi y}{b})e^{i\omega t}, \quad (89)$$

$$\phi_x(x,y,t)=\psi_{x0}\cos(\frac{n\pi x}{L})\sin(\frac{m\pi y}{b})e^{i\omega t}, \quad (90)$$

$$\phi_y(x,y,t)=\psi_{y0}\sin(\frac{n\pi x}{L})\cos(\frac{m\pi y}{b})e^{i\omega t}, \quad (91)$$

$$\varphi(x,y,t)=\varphi_0\sin(\frac{n\pi x}{L})\cos(\frac{m\pi y}{b})e^{i\omega t}, \quad (92)$$

where n and m are axial and lateral mode numbers, respectively; ω is the structure frequency. Substituting Eqs. (87)-(92) into Eqs. (79)-(84) yields

$$\begin{bmatrix} K_{11} & K_{12} & K_{13} & K_{14} & K_{15} & K_{16} \\ K_{21} & K_{22} & K_{23} & K_{24} & K_{25} & K_{26} \\ K_{31} & K_{32} & K_{33} & K_{34} & K_{35} & K_{36} \\ K_{41} & K_{42} & K_{43} & K_{44} & K_{45} & K_{46} \\ K_{51} & K_{52} & K_{53} & K_{54} & K_{55} & K_{56} \\ K_{61} & K_{62} & K_{63} & K_{64} & K_{65} & K_{66} \end{bmatrix} \begin{bmatrix} u_0 \\ v_0 \\ w_0 \\ \psi_{x0} \\ \psi_{y0} \\ \varphi_0 \end{bmatrix} = 0, \quad (93)$$

Finally, for calculating the frequency of the system (ω), the determinant of matrix in Eq. (93) should be equal to zero.

4. Numerical results and discussion

A computer program is prepared for the vibration smart control solution of plate reinforced with Carbon nanotubes and piezoelectric layer. Here, poly vinilidene fluride (PVDF) is selected for the piezoelectric layer with the material properties of Table 1 (Kolahchi *et al.* 2016).

Table 1 Material properties of PVDF

Properties	PVDF	
C_{11}	238.24	(GPa)
C_{12}	3.98	(GPa)
C_{22}	23.6	(GPa)
e_{11}	-0.135	(C/m^2)
e_{12}	-0.145	(C/m^2)
ϵ_{11}	1.1e-8	(C^2/Nm^2)
ρ^P	5300	(kg/m^2)

Table 2 Hill's constants and density

Parameter	Unit	Value
k_r	**GPa**	30
l_r	**GPa**	10
m_r	**GPa**	1
n_r	**GPa**	450
p_r	**GPa**	1
ρ_r	**Kg/m³**	2300
ρ_m	**Kg/m³**	2500

In addition, polymer plate has Young's modulus of $E_m=70\,GPa$ and Poisson's ratio of $\nu_r=0.3$ which is reinforced by nanotube with density and Hill's constants shown in Table 2. In addition, shear correction factor is chosen 5/6 (Kolahchi *et al.* 2016).

4.1 Validation

In this paper, to validate the results, the frequency of the structure is obtained by assuming the absence of elastic medium ($K_w=0$). Therefore, all the mechanical properties and type of loading are the same as Whitney (1987). So the non-dimensional frequency is considered as $\Omega=\sqrt{\frac{\rho h\omega^2L^4}{D_0}}$ in which $D_0=E_1h^3/(12(1-\nu_{12}\nu_{21}))$. The results are compared with five references which have used different solution method. The exact solution is used by Whitney (1987) while discrete singular convolution approach is applied by Secgin and Sarigul (2008). The numerical solution method of Dai *et al.* (2004), Chen *et al.* (2003), Chow *et al*. (1992) are mesh-free, finite element and Ritz, respectively. As it is observed in Table 2, the results of present work are in accordance with the mentioned references.

4.2 Effects of different parameters

Fig. 2 illustrates the effect of the Carbon nanotubes volume fraction on the dimensionless frequency of structure ($\Omega=\omega L\sqrt{\rho_m/E_m}$) for length to thickness ratio (*L/h)* of 5,

Table 3 Validation of present work with the other references

Method	Mode number			
	1	2	3	4
Whitney (1987)	15.171	33.248	44.387	60.682
Secgin and Sarigul (2008)	15.171	33.248	44.387	60.682
Dai *et al.* (2004)	15.17	33.32	44.51	60.78
Chen *et al*. (2003)	15.18	33.34	44.51	60.78
Chow *et al.* (1992)	15.19	33.31	44.52	60.79
Present	15.169	33.241	44.382	60.674

length to width ratio (L/b) of 1 and piezoelectric thickness (h_p) of 0.04 m. It can be seen that with increasing the values of Carbon nanotubes volume fraction, the frequency of the system is increased. This is due to the fact that the increase of Carbon nanotubes leads to a harder structure. However, it may be concluded that using nanotechnology for reinforce of plates has an important role in improving the vibration behavior of system.

Fig. 3 shows the effect of Carbon nanotubes agglomeration on the dimensionless frequency of structure versus external applied voltage for c_r=1%, L/h= 5, L/b=1 and h_p=0.04 m. As can be seen, considering agglomeration of Carbon nanotubes leads to lower frequency. It is due to this point that the agglomeration of Carbon nanotubes decreases the stability and homogeneity of the structure.

The dimensionless frequency of the nano-composite plate is demonstrated in Fig. 4 for different elastic mediums for c_r=1%, L/h= 5, L/b=1, h_p=0.04 m and Winkler constant of K_w=100 GPa. As can be seen, considering elastic medium increases the frequency of the structure.

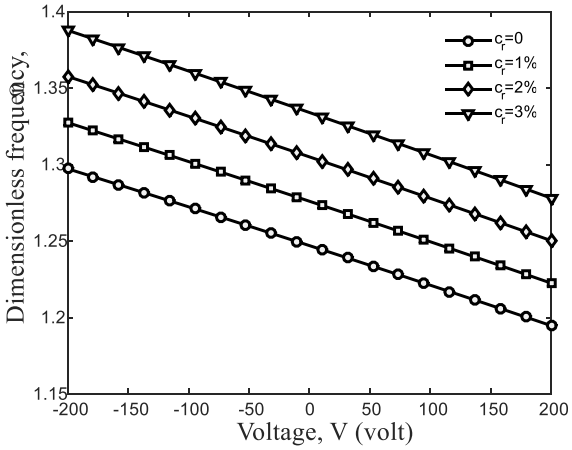

Fig. 2 Effects of Carbon nanotubes volume percent on the dimensionless frequency versus dimension applied voltage external

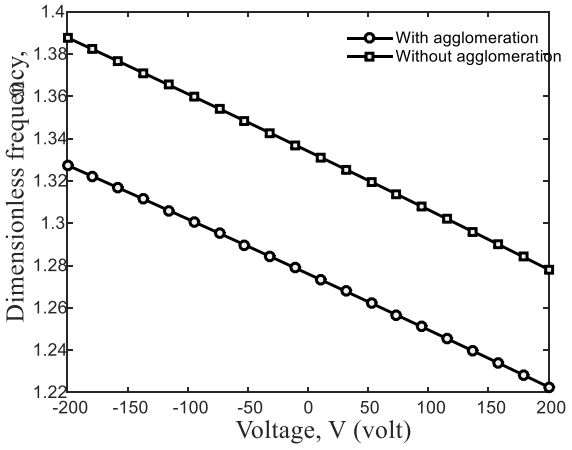

Fig. 3 Effects of Carbon nanotubes agglomeration on the dimensionless frequency versus dimension external applied voltage

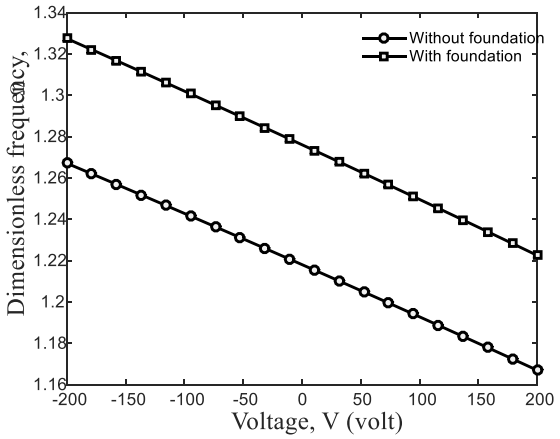

Fig. 4 Effects of elastic medium on the dimension frequency versus dimension external applied voltage

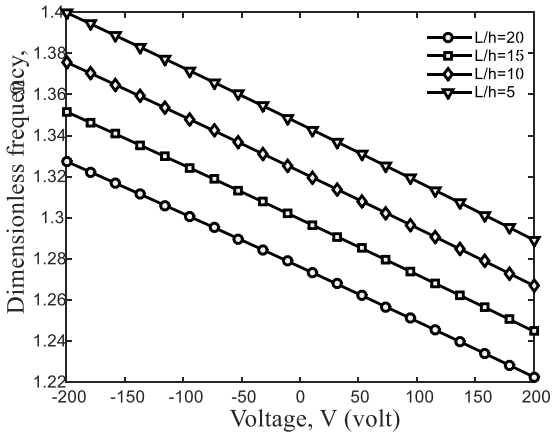

Fig. 5 Effects of length to thickness ratio of plate on the dimensionless frequency versus dimension external applied voltage

It is due to the fact that considering elastic medium leads to stiffer structure.

Furthermore, the frequency of the dense sand medium is higher than other cases since the spring constant of this medium is maximum.

The effect of the length to thickness ratio of plate on the dimensionless frequency of the system is depicted in Fig. 5 for c_r=0.05%, L/b=1 and h_p=0.04 m. As can be seen, the frequency of the structure decreases with increasing the length to thickness ratio. It is because increasing the length to thickness ratio leads to softer structure.

Fig. 6 shows the dimensionless frequency of the structure for different length to width ratio of the plate for c_r=1%, L/h= 5, and h_p=0.04 m. It can be also found that the frequency of the structure decrease with increasing the length to width ratio which is due to the higher stiffness of system with lower length to width ratio.

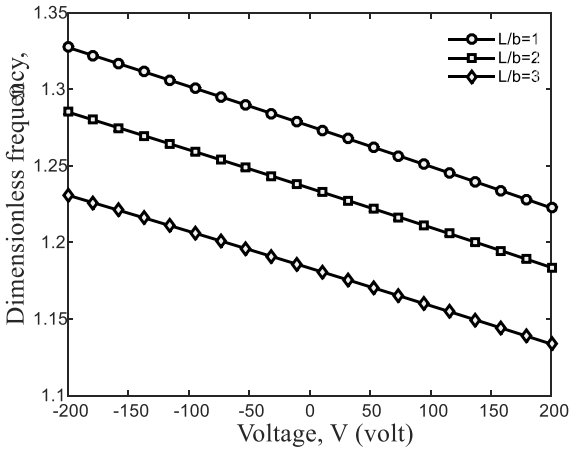

Fig. 6 Effects of length to width ratio of plate on the dimensionless frequency versus dimension external applied voltage

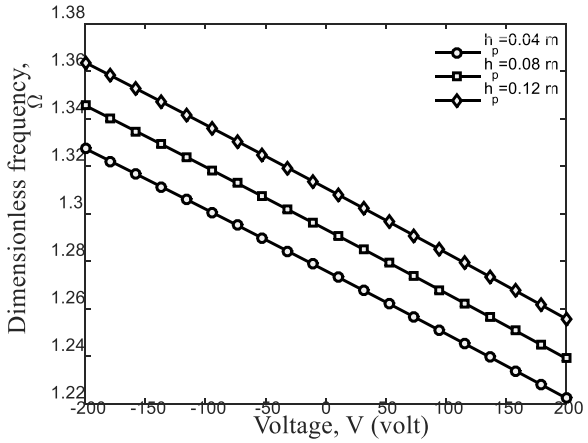

Fig. 7 Effects of piezoelectric layer thickness on the dimensionless frequency versus dimension external applied voltage

The effect of piezoelectric layer thickness on the dimensionless frequency is shown in Fig. 7 for c_r=1%, L/h= 5 and L/b=1. It can be found that with increasing the piezoelectric layer thickness, the frequency of the structure is increased. It is because with increasing the piezoelectric layer thickness, the stiffness of the structure will be improved.

4. Conclusions

Vibration smart control of embedded plates reinforced with Carbon nanotubes and covered with a piezoelectric layer subjected to external voltage was the main contribution of the present paper. Mori-Tanaka model is used for obtaining the effective material properties of the structure considering agglomeration effects. The elastic medium was simulated by Winkler foundation. Based on orthotropic FSDT, the motion equations were derived using energy method and Hamilton's principle. Exact solution is applied for obtaining the frequency of system so that the effects of the applied voltage, volume percent and agglomeration of Carbon nanotubes, elastic medium and geometrical parameters of plate were considered. It can be seen that with increasing the values of Carbon nanotubes volume fraction, the frequency of the system was increased. Considering agglomeration of Carbon nanotubes leads to lower frequency. It can be seen that considering elastic medium increases the frequency of the structure. In addition, the frequency of the structure decreases with increasing the length to thickness ratio and length to width ratio of the plate. It can be found that with increasing the piezoelectric layer thickness, the frequency of the structure was increased. Present results are in good agreement with those reported by the other references. Finally, it is hoped that the results presented in this paper would be helpful for control and design of plates.

References

Akgöz, B. (2019), "Static stability analysis of axially functionally graded tapered micro columns with different boundary conditions", *Steel Compos. Struct.*, **33**(1), 965-974. https://doi.org/10.12989/scs.2019.33.1.965.

Bahmyari, E. and Khedmati, M.R. (2013), "Vibration analysis of nonhomogeneous moderately thick plates with point supports resting on Pasternak elastic foundation using element free Galerkin method", *Eng. Anal. Bound. Elem.*, **37**(10), 1212-1238. https://doi.org/10.1016/j.enganabound.2013.05.003.

Bowles, J.E. (1988), *Foundation analysis and design*, Mc Graw Hill Inc..

Chahar, R.S. and Kumar, R.B. (2019), "Effectiveness of piezoelectric fiber reinforced composite laminate in active damping for smart structures", *Steel. Compos. Struct.*, **31**(4), 555-564. https://doi.org/10.12989/scs.2019.31.4.387.

Chen, J., Li, P., Song, G. and Ren, Z. (2016), "Piezo-based wireless sensor network for early-age concrete strength monitoring", *Optik*, **127**(5), 2983-2987. https://doi.org/10.1016/j.ijleo.2015.11.170.

Chen, S.S., Liao, K.H. and Shi, J.Y. (2016), "A dimensionless parametric study for forced vibrations of foundation-soil systems", *Comput. Geotech.*, **76**, 184-193. https://doi.org/10.1016/j.compgeo.2016.03.012.

Chen, X.L., Liu, G.R. and Lim, S.P. (2003), "An element free Galerkin method for the free vibration analysis of composite laminates of complicated shape", *Compos. Struct.*, **59**(2), 279-289. https://doi.org/10.1016/S0263-8223(02)00034-X.

Chow, S.T., Liew, K.M. and Lam, K.Y. (1992), "Transverse vibration of symmetrically laminated rectangular composite plates", *Compos. Struct.,***20**, 213-226. https://doi.org/10.1016/0263-8223(92)90027-A.

Dai, K.Y., Liu, G.R., Lim, M.K. and Chen, X.L. (2004), "A mesh-free method for static and free vibration analysis of shear deformable laminated composite plates", *J. Sound Vib.*, **269**, 633-652. https://doi.org/10.1016/S0022-460X(03)00089-0.

De Rosa, M.A. and Lippiello, M. (2009), "Free vibrations of simply supported double plate on two two models of elastic soils", Int. J. Num. Anal. Meth. Geomech. 33, 331-353. https://doi.org/10.1002/nag.717.

Dutta, G., Singh V.K., Mahapatra, T.R. and Panda S.K. (2017), "Electro-magneto-elastic response of laminated composite plate: A finite element approach", *Int. J. Appl. Computat. Math*., **3**(3), 2573-2592. https://doi.org/10.1007/s40819-016-0256-6.

Ferreira, A.J.M., Roque, C.M.C., Neves, A.M.A., Jorge, R.M.N.

and Soares, C.M.M. (2010), "Analysis of plates on Pasternak foundations by radial basis functions", *Comput. Mecch.*, **46**, 791-803. https://doi.org/10.1007/s00466-010-0518-9.

Ebrahimi. F., Jafari, A. and Barati, M.R. (2017), "Vibration analysis of magneto-electro-elastic heterogeneous porous material plates resting on elastic foundations", *Thin Wall. Struct.*, **119**, 33-46. https://doi.org/10.1016/j.tws.2017.04.002.

Hosseini-Hashemi, Sh., Rokni Damavandi Taher, H., Akhavan, H. and Omidi, M. (2010), "Free vibration of functionally graded rectangular plates using first-order shear deformation plate theory", *Appl. Math. Model.,* **34**, 1276-1291. https://doi.org/10.1016/j.apm.2009.08.008.

Kolahchi, R., Hosseini, H. and Esmailpour, M. (2016), "Differential cubature and quadrature-Bolotin methods for dynamic stability of embedded piezoelectric nanoplates based on visco-nonlocal-peizoelasticity theories", *Compos. Struct*., **157**, 174-186. 10.1016/j.compstruct.2016.08.032.

Kumar, Y. and Lal, R. (2012), "Vibrations of nonhomogeneous orthotropic rectangular plates with bilinear thickness variation resting on Winkler foundation", *Meccanica*, **47**, 893-915, https://doi.org/10.1007/s11012-011-9459-4.

Lam, K.Y., Wang, C.M. and He, X.Q. (2000), "Canonical exact solutions for levy-plates on two-parameter foundation using green's functions", *Eng. Struct.*, **22**, 364-378. https://doi.org/10.1016/S0141-0296(98)00116-3.

Mantari, J.L., Granados, E.V. and Guedes Soares, C. (2014), "Vibrational analysis of advanced composite plates resting on elastic foundation", *Compos. Part B-Eng.*, **66**, 407-419. https://doi.org/10.1016/j.compositesb.2014.05.026.

Meftah, A., Bakora, A., Zaoui, F.Z., Tounsi A. and Adda Bedia E.A. (2017), "A non-polynomial four variable refined plate theory for free vibration of functionally graded thick rectangular plates on elastic foundation", *Steel Compos. Struct*., **23**(3), 317-330. https://doi.org/10.12989/scs.2017.23.3.317.

Medani, M., Benahmed, A., Zidour, M., Heireche, H., Tounsi, A., Anis Bousahla, A., Tounsi, A. and Mahmoud, S.R. (2019), Static and dynamic behavior of (FG-CNT) reinforced porous sandwich plate using energy principle", *Steel Compos. Struct.*, **32**(5), 595-610. https://doi.org/10.12989/scs.2019.32.5.595.

Mehar K., Mahapatra, T.R., Panda, S.K. and Katariya, P.V. (2018), "Finite-element solution to nonlocal elasticity and scale effect on frequency behavior of shear deformable nanoplate structure", *J. Eng. Mech*., **144**, 04018094. https://doi.org/10.1061/(ASCE)EM.1943-7889.0001519.

Mehar K. and Panda, S.K. (2019), "Multiscale modeling approach for thermal buckling analysis of nanocomposite curved structure", *Adv. Nano Res.*, **7**, 181-190. https://doi.org/10.12989/anr.2019.7.3.181.

Mori, T. and Tanaka, K. (1973), "Average stress in matrix and average elastic energy of materials with misfitting inclusions", *Acta Metall. Mater*., **21**, 571-574. https://doi.org/10.1016/0001-6160(73)90064-3.

Reddy, J.N. (2003), "Mechanics of laminated composite plates and shells: theory and analysis", 2nd Ed., CRC Press.

Sasmal, S., Ravivarman, N., Sindu, B.S. and Vignesh, K. (2017), "Electrical conductivity and piezo-resistive characteristics of CNT and CNF incorporated cementitious nanocomposites under static and dynamic loading", *Compos. Part A - Appl. S*., **100**, 227-243. https://doi.org/10.1016/j.compositesa.2017.05.018.

Secgin, A. and Sarigul, A.S. (2008), "Free vibration analysis of symmetrically laminated thin composite plates by using discrete singular convolution (DSC) approach: algorithm and verification", *J. Sound Vib*., **315**, 197-211. https://doi.org/10.1016/j.jsv.2008.01.061.

Shi, D.L. and Feng X.Q. (2004), "The Effect of nanotube waviness and agglomeration on the elastic property of carbon nanotube-reinforced composites", *J. Eng. Mater-T. ASME*, **126**, 250-270, https://doi.org/10.1115/1.1751182.

Shooshtari, A. and Razavi, S. (2015), "Large amplitude free vibration of symmetrically laminated magneto-electro-elastic rectangular plates on Pasternak type foundation", *Mech. Res. Commun.*, **69**, 103-113. https://doi.org/10.1016/j.mechrescom.2015.06.011.

Suman, S.D., Hirwani, C.K., Chaturvedi, A. and Panda. S.K. (2017), "Effect of magnetostrictive material layer on the stress and deformation behaviour of laminated structure", *IOP Conf. Series: Mat. Sci. Eng.*, **178** (1), 012026.

Singh, V.K. and Panda, S.K. (2015a), "Large amplitude free vibration analysis of laminated composite spherical shells embedded with piezoelectric layers", *Smart Struct. Syst*., **16**(5), 853-872. DOI: https://doi.org/10.12989/sss.2015.16.5.853.

Singh, V.K. and Panda, S.K. (2015b), "Geometrical nonlinear free vibration analysis of laminated composite doubly curved shell panels embedded with piezoelectric layers", *J. Vib. Cont.,* **23**, 2078-2093. https://doi.org/10.1177/1077546315609988.

Singh, V.K. and Panda, S.K. (2016), "Numerical investigation on nonlinear vibration behavior of laminated cylindrical panel embedded with PZT layers", *Procedia Eng.*, **144**, 660-667, https://doi.org/10.1016/j.proeng.2016.05.062.

Singh, V.K., Mahapatra, T.R. and Panda, S.K. (2016a), "Nonlinear transient analysis of smart laminated composite plate integrated with PVDF sensor and AFC actuator", *Compos. Struct.*, **157**, 121-130. https://doi.org/10.1016/j.compstruct.2016.08.020.

Singh, V.K., Mahapatra, T.R. and Panda, S.K. (2016b), "Nonlinear flexural analysis of single/doubly curved smart composite shell panels integrated with PFRC actuator", *Eur. J. Mech.-A/Solids*, **60**, 300-314. https://doi.org/10.1016/j.euromechsol.2016.08.006.

Uğurlu, B. (2016), "Boundary element method based vibration analysis of elastic bottom plates of fluid storage tanks resting on Pasternak foundation", *Eng. Anal. Bound. Elem*., **62**, 163-176, https://doi.org/10.1016/j.enganabound.2015.10.006.

Whitney, J.M. (1987), "*Structural analysis of laminated anisotropic plates*", Technomic Publishing Company Inc, Pennsylvania, USA.

CC